

Seasonal Change Investigation of Water Area in Lake Sakata Based on POLSAR Image Analysis

Ryoichi Sato ¹, Yuki Yajima ², Yoshio Yamaguchi ³ and Hiroyoshi Yamada ³

¹ Faculty of Education and Human Sciences, Niigata University

8050, 2-no-cho, Ikarashi, Niigata, 950-2181 Japan

E-mail: sator@ed.niigata-u.ac.jp

² Graduate School of Science and Technology, Niigata University, Japan

³ Department of Information Engineering, Niigata University, Japan

Abstract

This paper examines seasonal change of the water area in Lake Sakata by using Polarimetric Synthetic Aperture Radar (POLSAR) image analysis. Statistical POLSAR image analysis is carried out for both X- and L-band data, based on a three-component scattering power decomposition method, where the decomposed components are surface scattering, double-bounce scattering and volume scattering components. From the results of the image analysis for the L-band POLSAR data acquired by Pi-SAR system, it is found that strong double-bounce scattering can be observed at the vicinity of the boundary region between water area and the surrounding emerged-plants area in early and middle summer seasons. To verify the generating mechanism of the double-bounce scattering, the Finite-Difference Time-Domain (FDTD) polarimetric scattering analysis is also executed for a simplified boundary model, which simulates the local boundary region around the lake and consists of lots of vertical thin dielectric pillars on a perfect electric conductor (PEC) plate or on a PEC and dielectric hybrid plate. Taking into account the polarimetric feature of the double-bounce scattering obtained by both the FDTD and POLSAR image analyses, one can distinguish the water area from the bush of the emerged-plants around the lake, even when the water area are concealed by emerged-plants and/or floating-leaved plants. Consequently, it is found that by using the proposed approach, one can estimate the water area seasonal change for the lake and the surrounding wetland.

1. INTRODUCTION

Lake Sakata, located in Niigata city, Japan, is one of the most beautiful sand dune lakes. The arrivals of many waterfowls can be observed every winter. Marshes surrounding the lake provide a comfortable environment for the waterfowls. So the lake and the surrounding area were designated as a Ramsar site [1] in 1996.

Sakata is a freshwater lake formed in the hollow region between sand dunes, and the freshwater is supplied only from spring water of the dunes and rainwater. There is no inflow from rivers into the lake, as seen in Fig.1. Hence,

it is very important to investigate the seasonal changes of the water area and water level. So far, some investigations on the seasonal water area change have been reported in Refs.[2]-[4]. For wide area water area survey, a method by analyzing aerial photographs has been utilized [4]. However, such investigation method depends on the weather, since fine aerial photographs cannot be taken in bad weather condition. Therefore, an alternative monitoring method, independent of the weather condition, may be required.

In this paper, we investigate seasonal change of the water area in Lake Sakata by using Polarimetric Synthetic Aperture Radar (POLSAR) image analysis. POLSAR is based on microwave remote sensing technology, so it can work well under any weather conditions. The classification method used here is based on scattering power decomposition on physical scattering nature [5]-[7]. In the well-known three-component decomposition method [5], total scattering contribution is decomposed into three scattering mechanisms as surface scattering, double-bounce scattering and volume scattering. By using the three-component decomposition scheme, we carry out statistical POLSAR image analysis for actual data (X- and L-band data), acquired by Pi-SAR (provided by JAXA and NICT, Japan). It is found from the decomposed results for early and middle summer seasons that the double-bounce scattering can be observed not only at the vicinity of the boundary between the lake and the surrounding emerged-plants, but also at some points inside the emerged-plants area. This double-bounce scattering may be caused by right angle structures composed of many vertical stems of the emerged-plants and flat water surface, and it is utilized as a marker for estimating the water area of the lake.

To verify the generating mechanism of the double-bounce scattering observed from the L-band images, by using the Finite-Difference Time-Domain (FDTD) method, polarimetric scattering analysis is also executed for a simplified boundary model, which simulates the local boundary region around the lake and consists of lots of vertical thin dielectric pillars on a perfect electric conductor (PEC) plate or on a PEC-dielectric hybrid plate. It is found from the FDTD analysis that similar strong double-bounce scattering is observed only for the former model with a PEC plate, that is, only for



Fig. 1: Overview of Lake Sakata

high water level case. Consequently, taking into account the polarimetric feature of the double-bounce scattering from the target region, one can distinguish the water area from the bush of the emerged-plants around the lake, even when the water area is concealed by emerged-plants and/or floating-leaved plants.

Section 2 briefly introduces the scattering matrix and the corresponding covariance matrix in POLSAR image analysis. In Sect. 3, some decomposed results of the POLSAR image analysis and the detailed considerations are provided. In Sect. 4, the generating mechanism of the double-bounce scattering discussed in Sect.3 is cleared by the FDTD polarimetric scattering analysis for simplified water-emergent boundary models.

2. POLSAR IMAGE ANALYSIS

To examine the seasonal water area change of the lake, we shall apply the scattered power decomposition method based on the three-component scattering model [5] to POLSAR data for Lake Sakata and the surrounding area. In this paper, let us simply show the decomposed procedure for the covariance matrix $\langle[C]\rangle$, whose components are obtained by elements of Sinclair scattering matrix as

$$\langle[S(HV)]\rangle = \begin{bmatrix} S_{HH} & S_{HV} \\ S_{VH} & S_{VV} \end{bmatrix} = \begin{bmatrix} a & c \\ c & b \end{bmatrix}, \quad (1)$$

where $S_{HV} = S_{VH} = c$ for back scattering case. The corresponding ensemble average covariance matrix $\langle[C]\rangle$ with the reflection symmetry condition $\langle S_{HH} S_{HV}^* \rangle \sim \langle S_{VV} S_{HV}^* \rangle \sim 0$ is given as

$$\langle[C]\rangle = \begin{bmatrix} \langle|a|^2\rangle & 0 & \langle ab^* \rangle \\ 0 & 2\langle|c|^2\rangle & 0 \\ \langle ba^* \rangle & 0 & \langle|b|^2\rangle \end{bmatrix} \quad (2)$$

$$= f_s \langle[C]\rangle_{surface} + f_d \langle[C]\rangle_{double} + f_v \langle[C]\rangle_{vol}, \quad (3)$$

where $\langle \cdot \rangle$ denotes the ensemble average in the data processing, $\langle[C]\rangle_{surface}$, $\langle[C]\rangle_{double}$ and $\langle[C]\rangle_{vol}$ are the covariance matrices for surface scattering, double-bounce scattering and volume scattering, respectively (See Fig.2). Also, f_s , f_d and f_v are the unknown deterministic coefficients for each scattering component. The deterministic algorithm for the unknowns f_s , f_d , f_v are shown in Fig.3. The present algorithm for the three-component scattering model is as same as that for the four-component scattering model of Refs.[6],[7] when the Helix scattering component f_c equals zero. According to the algorithm as in Fig.3, by choosing the appropriate matrices $\langle[C]\rangle_{surface}$, $\langle[C]\rangle_{double}$, $\langle[C]\rangle_{vol}$, the total scattered

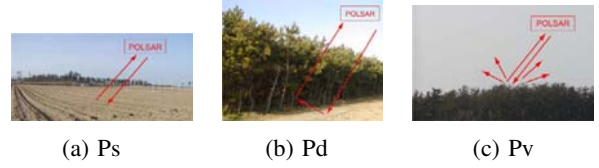


Fig. 2: Three scattering component model. (a) Surface scattering (P_s) (b) Double-bounce scattering (P_d) (c) Volume scattering (P_v)

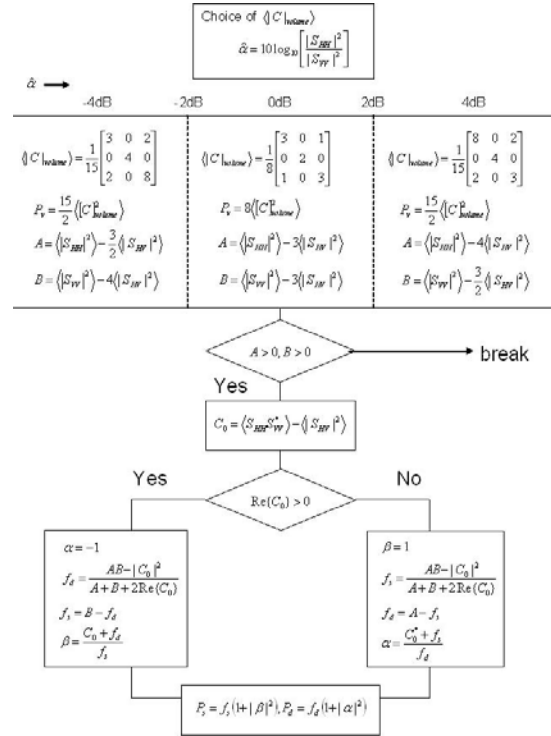
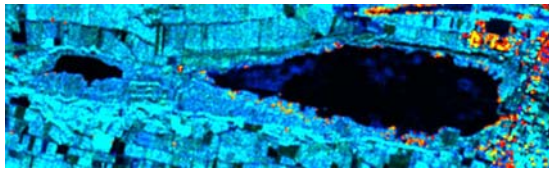


Fig. 3: A deterministic algorithm for the unknown coefficients f_s , f_d , f_v [5], [6].

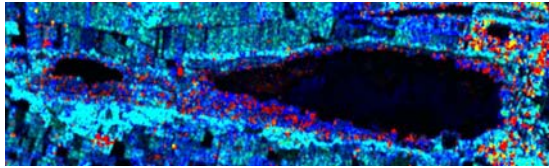
power can be successfully decomposed into each scattering component P_s , P_d , P_v .

3. RESULTS OF POLSAR ANALYSIS

Three scattering component decomposition method was applied to the POLSAR data around Lake Sakata acquired by PiSAR system, which is an airborne Polarimetric interferometric Synthetic Aperture Radar system developed by JAXA and NICT, Japan. Figure 4 shows the decomposed results for the POLSAR image data measured on June 13, 2002. Fig. 4(a) is the result at X-band (9.55 GHz), and Fig. 4(b) is at L-band (1.27 GHz). The resolution of each pixel and the average size are 1.5 m by 1.5 m and 10 by 10 pixels for X-band, and 3.0 m by 3.0 m and 5 by 5 pixels for L-band, respectively. In the figures, the decomposed scattering powers are color-coded as follows. 1) Blue color is painted for surface scattering P_s ,

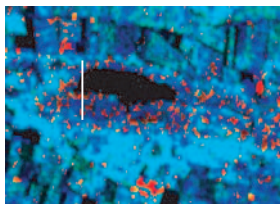


(a) X-band image on June 13, 2002

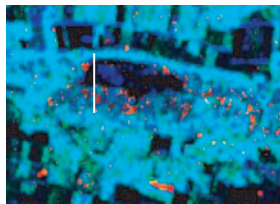


(b) L-band image on June 13, 2002

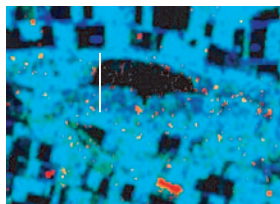
Fig. 4: Decomposed and color-coded images of Lake Sakata and the surrounding area



(a) June 13, 2002



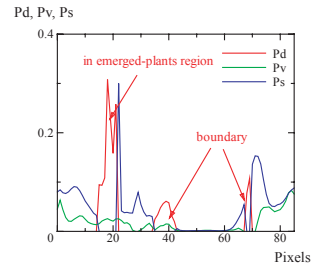
(b) August 4, 2004



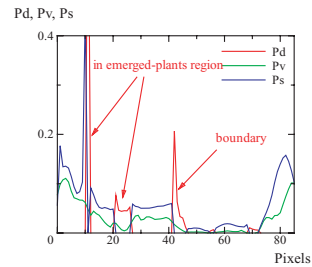
(c) November 3, 2004

Fig. 5: Decomposed and color-coded images of Kami-Sakata area

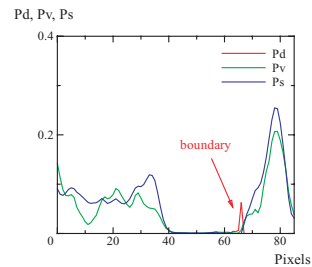
2) Red is for double-bounce scattering P_d , and 3) Green is for volume scattering P_v . As seen in Fig.4, the decomposed result for X-band has higher resolution than that for L-band on the whole. However, for the emerged-plants area around the water area, one can observe that the X-band image shows uniformly blue of surface scattering. This is due to the fact that the X-band wave cannot penetrate into the vegetation area, especially the emerged-plants area, so the scattering from the upper region (surface) of the emerged-plants is only observed. Hence, it may be unsuitable to survey the lower region under



(a) June 13, 2002



(b) August 4, 2004



(c) November 3, 2004

Fig. 6: Decomposed and color-coded results along a transect in Kami-Sakata area



Fig. 7: Spring water pools in emerged-plants area around Kami-Sakata area

the emerged-plants. While, most of the L-band wave can penetrate into the emerged-plants. Therefore, we will consider the polarimetric feature for the L-band images from now on.

Figure 5 shows the L-band decomposed and color-coded images around Kami-Sakata area. There are several red color spots for P_s at the surrounding region of the lake in early summer (a), and in middle summer (b). Such red spots (double-bounce scattering) are generally caused by man-made

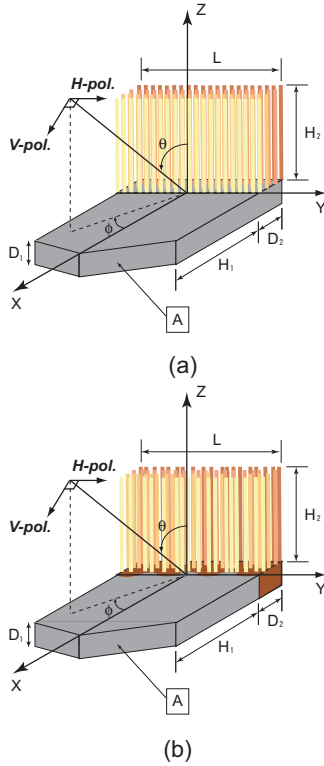


Fig. 8: Geometry of the problem (θ : look angle, ϕ : squint angle) (a) Vertical dielectric pillars on PEC plate (b) Vertical dielectric pillars on PEC-dielectric hybrid plate

structures [8]. For this case, the vertical stem of emerged-plants (reeds) and the water surface constitute dihedral corner reflector structures at the boundary of the lake, even though each emerged-plant is very thin (small) compared to the wavelength of the L-band wave. The dihedral structures may be finely constructed when the water level is high. For low water level case, fine dihedral structures are not made-up at the boundary. So the red color spot of the double-bounce scattering is hardly observed in autumn season of Fig.5 (c).

In Fig.6, to check the existence of the red spots in detail, let us show the decomposed results along the transect of Fig. 5. From Figs.6 (a) and (b), one can observe the red spots not only at the water-emergent boundaries but also inside the emergent regions. The latter double-bounce scattering of the red spots may be caused by the existence of the spring water pools inside the emergent (See Fig.7), that is, fine dihedral structures may be constructed by the water surface of the spring water pools and the emerged-plants. In next section, to verify this assumed scenario, we will carry out the polarimetric scattering analysis for simplified water-emergent boundary models by using the Finite-Difference Time-Domain (FDTD) method [9].

TABLE 1: PARAMETERS IN FDTD SIMULATION

Analytical region	350×350×350 cells
Cubic cell size Δ	0.01 m
Time step Δt	1.925×10^{-11} s
Incident pulse	Lowpass Gaussian pulse
Absorbing boundary condition	Mur 2nd

TABLE 2: FDTD STATISTICAL EVALUATION RESULTS OF THE POLARIMETRIC SCATTERING FROM THE BOUNDARY MODELS

Scattering component	Model (a)	Model (b)
P_s/P_t	0.17568	0.83320
P_d/P_t	0.81015	0.15831
P_v/P_t	0.01417	0.00849

4. FDTD POLARIMETRIC SCATTERING ANALYSIS

As depicted in Fig. 8, we will consider polarimetric scattering problem when H (horizontal) or V (vertical) linear polarized plane wave impinges on a simplified boundary model, which simulates the local boundary region around the lake and consists of lots of vertical thin dielectric pillars on a perfect electric conductor (PEC) plate (Model (a)) or on a PEC and dielectric hybrid plate (Model(b)). Model (a) simulates the vertical stems of the emerged-plants on water surface where the water level is assumed as high, and Model (b) is for low water level case that the emerged-plants are emerged near the boundary between soil ground and water area.

Here, the FDTD method [9] is utilized to obtain the scattering matrix for the models. The incident and squint angles are $\theta = \theta_i = 45^\circ$ and $\phi = \phi_i = 0^\circ$, respectively. Each dimension size of the scatterer is $L = 10.17\lambda$ (2.40 m), $H_1 = H_2 = 5.93\lambda$ (1.40 m), $D_1 = 2.54\lambda$ (0.60 m) and $D_2 = 3.60\lambda$ (0.85 m) at 1.27 GHz frequency, where a compensated trigonal part A is added to reduce the unnecessary back scattering from the horizontal edge of the front side. At 1.27GHz, the complex relative permittivity ϵ_{r1}^* for the thin dielectric pillars is set as $2.0 - j0.05$, and ϵ_{r2}^* for the dielectric part of the base plate in model (b) is $5.0 - j0.1$. The other fundamental parameters of the FDTD simulation used here are shown in Table 1.

In this paper, to evaluate statistical polarimetric scattering feature as actual POLSAR image analysis, the vertical pillars are randomly set on the plate, and the ensemble average processing are carried out for random 25 distributed patterns (snapshots) of the pillars. The results of the statistical evaluation are shown in Table 2. In the table, P_t is the total power as $P_t = P_s + P_d + P_v$. It is observed from the result for Model (a) that the dominant scattering contribution is P_d for the high water level case. On the other hand, for the low water level case of Model (b), the strong surface scattering is generated at the boundary between PEC (water) and dielectric (soil) parts. Taking into account the results of this FDTD statistical polarimetric scattering analysis, the following conclusion may be obtained

- P_d is dominant when water level is high. (from Model (a))
- P_s is major rather than P_d for low water level case. (from

Model (b))

5. CONCLUDING REMARKS

Seasonal change of the water area in Lake Sakata has been investigated by using POLSAR image analysis. Statistical POLSAR image analysis has been carried out for L-band data, based on a three-component scattering power decomposition method. Taking into account the polarimetric feature of the double-bounce scattering from the target region, one has been able to distinguish the water area from the bush of the emerged-plants around the lake when the water level is relatively high.

To verify the generating mechanism of the double-bounce scattering, the FDTD statistical polarimetric scattering analysis has also been executed for simplified water-ground boundary models, and the similar polarimetric feature for the double-bounce scattering has been observed by the simulation.

Therefore, by extracting the double-bounce scattering contribution from the entire image, one can easily classify the water area around the lake. This classification procedure can be suitable even for finding out the small spring water pools when most of the water area of the pool is concealed by emerged-plants and/or floating-leaved plants.

ACKNOWLEDGMENTS

The authors express their sincere appreciations to Professor H. Fukuhara for helpful discussions, and to JAXA and NICT, Japan, for providing valuable Pi-SAR image data around Lake Sakata. This research was partially supported by 2005 Niigata City Sakata Wetland Scientific Research Incentive Grant.

REFERENCES

- [1] Official Web site of the Ramsar Convention on Wetlands, <http://www.ramsar.org/index.html>
- [2] M. Nonaka *et al.*, "Nitrate movement through soil profile and ground-water pollution by nitrogen fertilizer in sand dune upland soil," *Jpn. J. Soil Sci. Plant Nutr.*, **67**, pp.633-639, 1996.
- [3] H. Fukuhara *et al.*, "Characteristics of nutrient dynamics in Lake Sagata, Japan, a shallow sand dune lake," *Hydrobiologia*, **506-509**, pp.93-99, 2003.
- [4] H. Fukuhara *et al.*, "Limnological studies of lakes in Niigata prefecture X. Changes in the area of emerged and floating-leaved plants, estimated by using aerial photographs, in Lake Sagata (Akatsuka, Niigata)," *Memoirs of the Faculty of Education and Human Sciences, Niigata University*, Vol.1, No.1, pp.1-15, Sept.1998.
- [5] A. Freeman and S. L. Durden, "A Three-component scattering model for polarimetric SAR data," *IEEE Trans. Geosci. Remote Sensing*, Vol.36, No.3, pp.963-973, May 1998.
- [6] Y. Yamaguchi *et al.*, "Four-Component Scattering Model for Polarimetric SAR Image Decomposition," *IEEE Trans. Geosci. Remote Sensing*, vol.43, No.8, Aug. 2005.
- [7] Y. Yamaguchi *et al.*, "A Four-Component Decomposition of POLSAR Images Based on the Coherency Matrix," *IEEE Geosci. Remote Sensing Letters*, vol.3, No.3, pp.292-296, July 2006.
- [8] K. Hayashi *et al.*, "Polarimetric Scattering Analysis for A Finite Dihedral Corner Reflector," *IEICE Trans. on Commun.*, Vol.E89-B, No.1, Jan. 2006.
- [9] A. Taflov *et al.*, *Computational Electrodynamics 2nd ed.*, Artech House, 2000.